Structural, Microstructural, and Electrical Transport Properties of TiO_2−RuO_2 Ceramic Materials Obtained by Polymeric Sol−Gel Route

M. T. Colomer* and J. R. Jurado

Instituto de Cerámica y Vidrio, CSIC, Antigua Ctra. Valencia Km. 24,300, 28500 Arganda del Rey, Madrid, Spain

Received June 17, 1999. Revised Manuscript Received November 30, 1999

Materials belonging to the $Ti_{1-x}Ru_xO_2$ system, where $0 \leq x \leq 1$ (mol), have been synthesized by a polymeric sol−gel route and calcined in air at 1300 °C by rapid firing. The crystalline evolution of the prepared materials has been investigated, as a function of temperature, by means of differential thermal analysis (DTA-TGA) and X-ray diffraction (XRD). Microstructures of the sintered materials were studied by scanning electron microscopy−energy-dispersive X-ray (SEM-EDX). Electrochemical impedance spectroscopy (EIS) and dc four-point methods were used to characterize electrically, in air, the ceramic materials obtained. For sintered materials, due to the partial volatilization of RuO_2, the x real values were obtained by X-ray fluorescence (XRF) chemical analysis. Although, from 300 to 500 °C the solid solubility of RuO_2 in rutile-TiO_2 phase is located at $x \geq 0.5$, from 600 to 1300 °C, that value is located in the $0.05 \leq x < 0.1$ range. For higher contents of RuO_2, two phases are observed: ruthenium−titanium oxide rutile solid solution and RuO_2. Two types of electrical behavior are detected in sintered materials of this system: semiconductor and metallic. A wide transition semiconductor/metal is noted, which indicates the existence of a prepercolation effect. The metal/electrical percolation can be located at a chemical analyzed composition of $x = 0.26$. On the other hand, a microstructural/electrical approach is considered.

I. Introduction

Metallic conductive oxides, like RuO_2, IrO_2, etc., have been well-known for many years to be very active catalysts in anodic processes such as Cl_2 and O_2 evolution or in O_2 cathodic reduction.[1−6] In addition, they possess both high electrical conductivity and electrochemical stability (up to 500 °C), especially the latter, when it is blended with other oxides.[7] The high electrocatalytical activity of these oxides for O_2 evolution is correlated with the appropriated value of the chemisortion energy for an oxygenated species. Furthermore, the capacity of RuO_2 to adsorb hydrogen reversibly may play an important role in CO_2 reduction.[8] Finally, RuO_2 is used as a catalyst in the Fischer−Tropsch conversion of carbon monoxide to either hydrocarbons or alcohols,[9] one of the most valuable systems for electrochemical applications is the ruthenium−titanium metallic oxides. They are generally prepared by thermal decomposition onto metallic titanium substrates. However, a variety of microanalyses have revealed that the surface composition and features of these electrodes are not homogeneous.[10−16] To clarify the physical properties of these electrocatalyts in detail and develop more extensive applications, it is desirable to establish new methods of preparing not only homogeneous coatings but also dispersible fine particles of the binary metal oxides. In this regard, the sol−gel process may be a good approach to prepare the oxide particles of this system and very little work has been found in the literature.[17,18] In any case, the advantage for using this technique is that one could find electrode structures which possess a uniform and homogeneous distribution of electrocatalytically

(1) Ogwura, K. *J. Appl. Electrochem*. **1986**, *16*, 732.
(2) de Nora, O. *Chem. Ing. Technol.* **1970**, *42*, 222.
(3) Trasatti, S.; Lodi, G. In *Electrodes of Conductive Metal Oxides*; Trasatti, S., Ed.; Elsevier: Amsterdam, 1980; p 301
(4) Kuhn, A. T.; Mortimer, C. S. *J. Electrochem. Soc.* **1973**, *120*, 231.
(5) Bandi, A.; Mihelis, A.; Vartires, I.; Ciortan, E.; Rosu, I. *J. Electrochem. Soc.* **1987**, *134*, 1982.
(6) Bandi, A.; Vartires, I.; Mihelis, A.; Hainaroise, C. *J. Electroanal. Chem*. **1983**, *157*, 241.
(7) Iwakura, C.; Inai, M.; Uemura, T.; Tamura, H. *Electrochim. Acta* **1981**, *26*, 579.
(8) Hepel, T.; Pollak, F. H.; O'Grady, W. E. *J. Electrochem. Soc.* **1984**, *131*, 2094.
(9) Morris, S. R.; Moyes, R. B.; Wells, P. B. In *Metal Support and Metal Additive Effects in Catalysis*; Imelik, B., Ed.; Elsevier: Amsterdam, New York, 1982; p 247.
(10) Gerrard, W. A.; Steele, B. C. H. *J. Appl. Electrochem*. **1978**, *8*, 417.
(11) Trasatti, S. *Electrochim. Acta* **1991**, *36*, 225.
(12) Pizzini, S.; Buzzanca, G.; Mari, C.; Rossi, L.; Torchio, S. *Mater. Res. Bull*. **1972**, *7*, 449.
(13) Augustynski, J.; Balsenic, L.; Hinden, J. *J. Electrochem. Soc.* **1978**, *125*, 1093.
(14) Lodi, G.; Asmundis, C. D.; Ardizzone, S.; Sivieri, E.; Trasatti, S. *Surf. Technol.* **1981**, *14*, 335.
(15) Battisti, A. D.; Lodi, G.; Cappadonia, M.; Battaglia, G.; Kotz, R. *J. Electrochem. Soc.* **1989**, *136*, 2596.
(16) Wagner, W.; Kuhnemund, L. *Cryst. Res. Technol.* **1989**, *24*, 1009.
(17) Guglielmi, M.; Colombo, P.; Rigato, V.; Battaglin, G.; Boscolo-Boscoletto, A.; DeBattisti, A. *J. Electrochem. Soc.* **1992**, *139*, 1655.
(18) Kameyama, K.; Shohji, S.; Onoue, S.; Nishimura, K.; Yahikozawa, K.; Takasu, Y. *J. Electrochem. Soc.* **1993**, *140*, 1034.

10.1021/cm9903879 CCC: $19.00
Published on Web 03/29/2000

active ruthenium points in all the electrode microstructure. That feature cannot be obtained by the conventional decomposition method.

Guglielmi et al.[17] have tried to apply a sol−gel method to preparing RuO_2-TiO_2 catalysts; however, they have not tried to obtain isolated fine particles of those oxides, but prepared multilayer coatings of those oxides on fused silica, with and without vacuum, by a spin-coating technique. The different samples contained a nominal composition of 30 mol % of RuO_2 and 70 mol % of TiO_2. Kameyama et al.[18] prepared ultrafine binary oxide particles of RuO_2-TiO_2 by a sol−gel process. It enabled them to obtain derived rutile-type solid solution oxides of ruthenium and titanium with well-defined stoichiometry, except for the Ti-rich oxide composition, which appears not to form a homogeneous solid solution.

Swider et al.[19] synthesized aerogels comprised of ruthenium dioxide−titanium dioxide [$(Ru-Ti)O_x$] to examine the effect of enhanced surface area on electrical properties. On the other hand, pyrolysis of mixtures of ruthenium hydrated chloride and Ti(IV) isopropoxide has been used to obtain films of TiO_2-RuO_2. De Battisti et al.[20] prepared RuO_2/TiO_2 mixed oxide films (20, 30, 50 70, 80, and 100 mol % of noble metal) by the mentioned method. The calcination temperature was 500 °C. Rutherford backscattering spectrometry (RBS) results confirmed segregation of TiO_2 species in the surface region of all the RuO_2/TiO_2 compositions.

Most of the research in this system, except the one by Hrovat et al.,[21] has been done at temperatures up to 500 °C, due to the volatilization of RuO_2 in air above 800 °C.[22] To increase the chemical and thermal stability of this oxide, it could be used as a matrix, which would accommodate and stabilize it. If this is so, it would allow higher operation temperatures and then enhance efficiency, for example, in the Fischer−Tropsch industrial process. Different attempts have been carried out into ZrO_2 and La_2O_3/ZrO_2,[23] and also into ZrO_2/Y_2O_3.[24,25]

The purpose of the present investigation is to obtain and characterize ceramic materials in the TiO_2-RuO_2 system prepared by a polymeric sol−gel method. In this paper, xerogels with nominal compositions $Ti_{1-x}Ru_xO_2$, where $x = 0$, 0.05, 0.10, 0.15. 0.20, 0.30, 0.50, and 1 (mol), were synthesized. After calcination, in the temperature range from 300 to 1300 °C, structural studies were carried out to determine the stability in air of the solid solutions as a function of the temperature. After rapid firing in air at 1300 °C, structural, microstructural, chemical, and electrical characterization of the ceramic compacts obtained were performed.

II. Experimental Section

Gels were prepared from Merck analytical grade ruthenium(III) acetylacetonate (acac) and 98% titanium(IV) isopropoxide purchased from Janssen, as described in the flowchart in Figure 1. In this method, absolute ethanol (Panreac) medium was used. Water was added as 3 M HNO_3. The molar ratios were titanium(IV) isopropoxide/H_2O = 1:1.5 and titanium(IV) isopropoxide/H^+ = 1:0.09.

In a first stage, the Ru(III)acac was dissolved in absolute ethanol, and the solution was refluxed and stirred at 70 °C for 72 h. Titanium(IV) isopropoxide was also dissolved in absolute ethanol, and the solution was refluxed and stirred at 70 °C for 72 h. After that, the latter solution was added to the Ru(III)acac solution and the mixture was refluxed and with continuous stirring at 70 °C for 72 h. Finally, 3 M HNO_3 was added as necessary to reach a titanium(IV) isopropoxide/H_2O ratio of 1:1.5.

To slow solvent evaporation, gels were dried very slowly by covering them with a plastic film. Holes were made in the film with a needle to control the speed of evaporation.[26] The xerogels were thermally treated at several temperatures between 200 and 1300 °C with 12 h of soaking time to study the crystalline evolution. The calcined powders at 700 °C were sieved at 35 μm and pressed (axial and isostatically). Pellets were sintered, in air at 1300 °C for 10 min by rapid firing, at a heating and cooling rate of 20 °C/min, to minimize volatilization losses. The furnace used was a Rapid High-Temperature Furnace (Bulten-Kanthal AB, S-73401 Hallstahammar, Sweden).

Differential thermal and thermogravimetric analyses (DTA-TGA) were carried out in a Perkin-Elmer thermoanalyzer under dry air, using platinum crucibles and a constant heating rate of 10 °C/min up to 1300 °C. Finely powdered alumina was used as a reference substance. Crystalline evolution was followed by XRD (Siemens D-5000 diffractometer) using Cu $K\alpha_1$ radiation and a Ni filter. Powder particles were easily deagglomerated by ultrasonication in isopropyl alcohol and particle sizes and morphologies of the as-prepared powders were estimated using transmission electron microscopy (TEM) (JEOL JEM-2010), after depositing a droplet of the alcoholic suspension onto a copper grid fitted with a cellulose-based film, drying, and Au/Pd coating. By means of scanning electron microscopy−energy-dispersive X-ray (SEM-EDX) (model DSM 950, Zeiss, Oberchen, Germany) the morphology of the calcined powders and the microstructure were observed. The microstructure of the sintered samples was analyzed on polished and chemically etched surfaces. Final densities were measured by the Archimedes immersion technique in water. To determine the intergranular porosity of the sintered bodies a Hg porosimeter Micromeritics Autopore II 92220 was used. Sintered samples were chemical analyzed by X-ray fluorescence (XRF). A Philips (model PW-1404) spectrometer with an X-ray tube: Sc/Mo double anode was used. The sintered samples were cut into disks and electroded for the electrical measurements. Impedance measurements were performed in air (at temperatures between 250 and 1000 °C) for $x = 0$ (platinum paste electrodes were used). For materials with $0 < x \leq 0.20$ mol RuO_2, sputtered gold electrodes were employed. The measurements were performed between room temperature and 500 °C, by using a computer-assisted impedance analyzer HP4192A, (frequency range of $10-10^7$ Hz). Samples with $x =$ 0.30, 0.50, and 1 mol RuO_2 were electrically measured by a dc four-terminal method. The sintered samples were cut into the shape of a parallelepiped, as current and voltage probes (four silver-paste electrodes) were fixed on it, in the temperature range from 77 to 373 K. A cryostat (Oxford Instruments, model DN 1710), a Tektronix PS280 source, and two multimeters (HP34401A) were employed.

In the following, $Ti_{1-x}Ru_xO_2$ will be labeled $100(1-x)T100xR$.

III. Results and Discussion

The conventional solid-state reaction was also tested in this work to obtain ceramic materials with the

(19) Swider, K. E.; Merzbacher, C. I.; Hagans, P. L.; Rolison, D. R. *Chem. Mater.* **1997**, *9*, 1248.

(20) De Battisti, A.; Battaglin, G.; Benedetti, A.; Kristof, J.; Liszi, J. *Chimia* **1995**, *49*, 17.

(21) Hrovat, M.; Holc, J.; Samardizja, Z.; Drazic G. *J. Mater. Res.* **1996**, *11*, 727.

(22) Tagirov, V. K.; Chizhikov, D. M.; Kazenas, E. K.; Shubocchkin, L. K. *J. Inorg. Chem.* **1977**, *20*, 1133.

(23) Long, Y. C.; Zhang, Z. D.; Dwight, K.; Wold, A. *Mater. Res. Bull.* **1988**, *23*, 631.

(24) Djurado, E.; Roux, C.; Hammou, A. *J. Eur. Ceram. Soc.* **1996**, *16*, 767.

(25) Colomer, M. T.; Jurado, J. R. *J. Non-Cryst. Solids* **1997**, *217*, 48.

(26) Zarzycki, J.; Prassas, M.; Phalippou, J. *J. Mater. Sci.* **1982**,*17*, 3371.

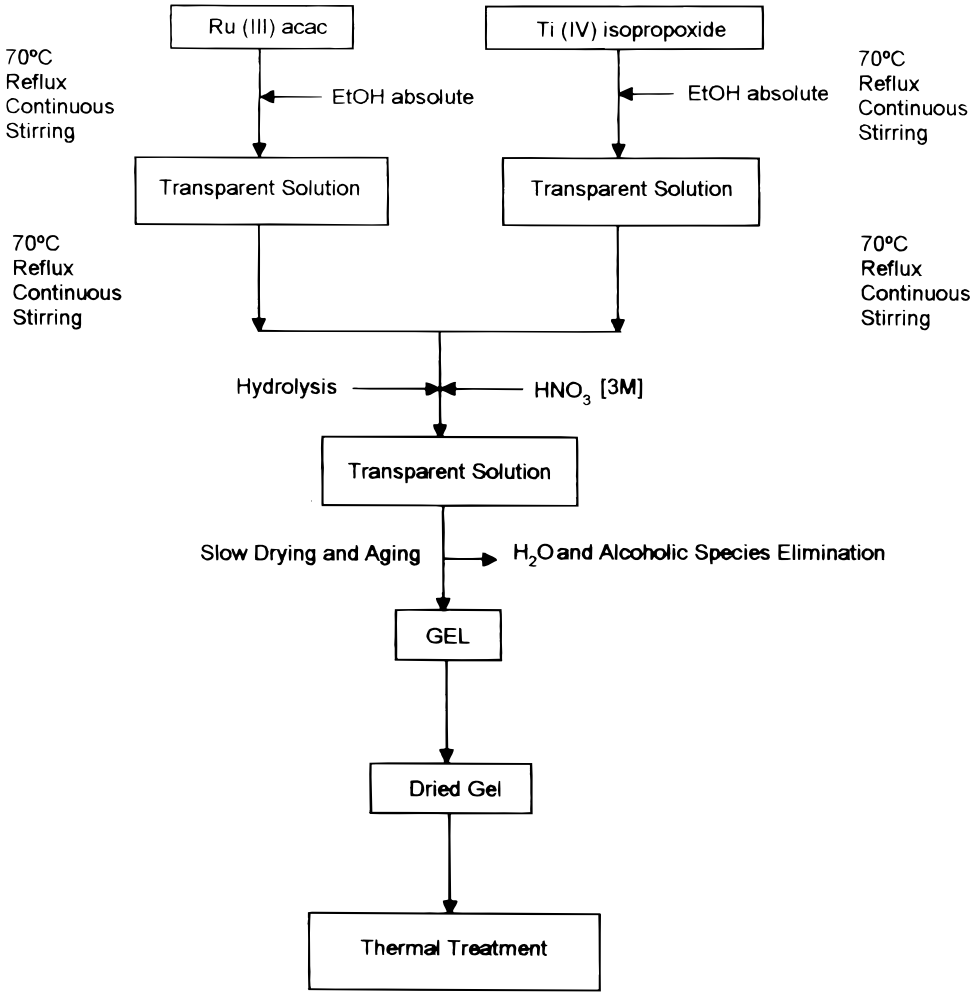

Figure 1. Flowchart of the synthesis of TiO_2−RuO_2 xerogels.

described composition. Despite the use of a $RuO_3 + RuO_4$-rich atmosphere (buffer) and rapid firing, the samples obtained after sintering between 1000 and 1300 °C exhibited high porosity, and according to the XRD analysis, any related ruthenium phases were not detected (due to the complete volatilization of RuO_2).

A. DTA-TGA Analysis. All the TGA curves show strong weight losses up to 420 °C (32% for 70T30R) and are associated with the evaporation of water and alcohols and the combustion of the organic material.[27] All the DTA and TGA curves exhibit similar characteristics in the temperature range 920−1300 °C, except for the 95T5R and 100T samples. In that temperature range, weight losses were detected (1.19% for 70T30R), which is likely due to the RuO_2 partial volatilization (as RuO_3 and RuO_4) that does not enter in rutile−TiO_2 solid solution. RuO_2 and the rutile solid solution (Ti−Ru)O_2 crystalline phases were detected in the residual ash, by means of XRD. The DTA analyses showed as their salient features exothermic peaks centered at 300 and 1070 °C (70T30R), which were attributed to the combustion of the organic material and the volatilization process, respectively.

In the 95T5R and 100T compositions, no weight loss is detected in the 920−1300 °C temperature interval. On the other hand, the RuO_2 volatilization process is enhanced when RuO_2 content is higher in the material.

B. XRD Studies. Crystalline Phase Evolution. The extent of the solid solubility in this system is a controversial matter in the literature. Gerrard and Steele[10] reported the presence of a very limited solid solubility (<1.5% mol RuO_2) at 800 °C. They used the conventional thermal decomposition method for the synthesis. Guglielmi et al.[17] reported that for 30 mol % RuO_2, at 400 °C, a rutile solid solution is formed which agrees well with this work. They used a sol−gel method for the synthesis and did not study the phase evolution at higher temperatures. Kameyama et al.[18] obtained a rutile solid solution phase at 450 °C for compositions with high content of RuO_2 (80% at.) but no solid solution of RuO_2 into TiO_2 was attained for compositions with less than 20% at. of RuO_2. These authors also did not investigate higher temperatures in their work.

On the other hand, Hrovat et al.[21] used wavelength-dispersive X-ray quantitative microanalysis (WDS) for the investigation of phase equilibria and the extent of solid solubility in the RuO_2−TiO_2 system (the conventional ceramic method was used for the synthesis and the pellets were buried in RuO_2 powder to suppress the evaporation of volatile RuO_3 and RuO_4). These authors reported a solid solubility of RuO_2 in TiO_2 of about 0.094 mol at 1300 °C. The solid solubility at 1350 °C was determined to be 0.165 mol TiO_2 in RuO_2 and 0.135 mol

(27) Colomer, M. T.; Jurado, J. R. *J. Solid State Chem.* **1998**, *141*, 282.

Table 1. Evolution of the Crystalline Phases for $0 \le x \le 0.50$ in the TiO_2-RuO_2 as a Function of the Temperature[a]

calcination temperature (°C)	$x = 0$	$x = 0.05$	$x = 0.10$	$x = 0.15$	$0.20 \le x \le 0.50$
300	TA	↑TA + Rss↓	↑TA + Rss↓	↑TA + Rss↓	↑TA + Rss↓
400	TA	↑TA + Rss↓	↑TA + Rss↓	↑TA + Rss↓	↑TA + Rss↓
500	↓TA + TR↑	↑TA + Rss↓	↑TA + Rss↓	↑TA + Rss↓	↓TA[b] + Rss↑
600	↓TA + TR↑	↓TA + Rss↑	↓TA + ↑Rss + R↓	↑Rss + R↓	↑Rss + R↓
700	TR	Rss	↑Rss + R↓	↑Rss + R↓	Rss + R[c]
1300	TR	Rss	↑Rss + R↓	↑Rss + R↓	Rss + R2

[a] Anatase is labeled TA, rutile is TR, and the rutile solid solution phase $(Ti-Ru)O_2$ is Rss, and RuO_2 is R. The up arrow (↑) indicates highest intensity peaks and the down arrow (↓) indicates weak intensity of the diffraction peaks, respectively. [b] For $x = 0.50$ anatase is not detected. [c] For $x \ge 0.30$, at temperatures higher than 700 °C; the phase evolution runs to obtain similar concentration of both, Rss and R.

RuO_2 in TiO_2. They claimed an increment of the solubility as firing temperature is raised from 900 to 1350 °C. It is not in accord with this work where the extent of solid solubility shows an opposite trend than that proposed by Hrovat et al.[21]

The extent and the temperature dependence of solid solubility from 300 to 1300 °C is investigated in this system (12 h of soaking time at each temperature). Table 1 shows the crystalline phases detected in samples with $0 \le x \le 0.50$ and their evolution with temperature. Anatase is labeled TA, rutile is TR, the rutile solid solution phase $(Ti-Ru)O_2$ is Rss, and RuO_2 is R.

Rss peaks could be assigned to a rutile structure with *d* spacings shifted with respecting to rutile−TiO_2 phase (except for the sample with $x = 0$). A separation between the $(Ti-Ru)O_2$ and RuO_2 phases was observed with increasing calcination temperature (from 600 °C).The diffraction peaks of the solid solution were shifted to the peaks of TiO_2. This shift suggests that part of Ru^{4+} is excluded from the $(Ti-Ru)O_2$ lattice at temperatures greater than 600 °C. Ito et al.[28] found a similar trend in the system RuO_2-SnO_2. The solid solution of RuO_2 in SnO_2 was stable only up to 600 °C. The difference between both systems is that in the TiO_2-RuO_2 system there is still a solid solution above 600 °C. Although, from 300 to 500 °C, the solid solubility of RuO_2 in TiO_2 is located at $x \ge 0.50$, from 600 to 1300 °C, that value is located in the $0.05 \le x < 0.10$ range. The diminution of the solid solubility probably indicates that the RuO_2 oxidation reaction starts at lower temperatures than that of 800 °C reported by Tagirov et al.[22]

The absence of a significant solid solution between RuO_2 and TiO_2 may appear surprising since the constituent oxides appear to satisfy the requirements of the Hume−Rothery rules for solid solution formation. However, the electronic band structures and lattice properties of the two oxides differ considerably. For example, deviations from stoichiometry are accommodated in TiO_2 by the formation of crystallographic shear planes, whereas there is no evidence for similar defects in nonstoichiometric RuO_2.[29] It is clear that the RuO_2 oxidation reaction[22] implies as well that trend. RuO_2 oxidation could enhance the absence of a significant solid solution.

One remarkable effect is that RuO_2 catalyzes the anatase−rutile transformation.[10,30] As the RuO_2 content increases, the transformation temperature decreases (see Table 1). That fact occurs in a similar way when Ti or Pt metallic substrates are used to deposit RuO_2-TiO_2 products or in the SnO_2-TiO_2 system.[28] It agrees well with the results reported by Gerrard and Steele,[10] Veseloskaya et al.,[30] and Hine et al.[31]

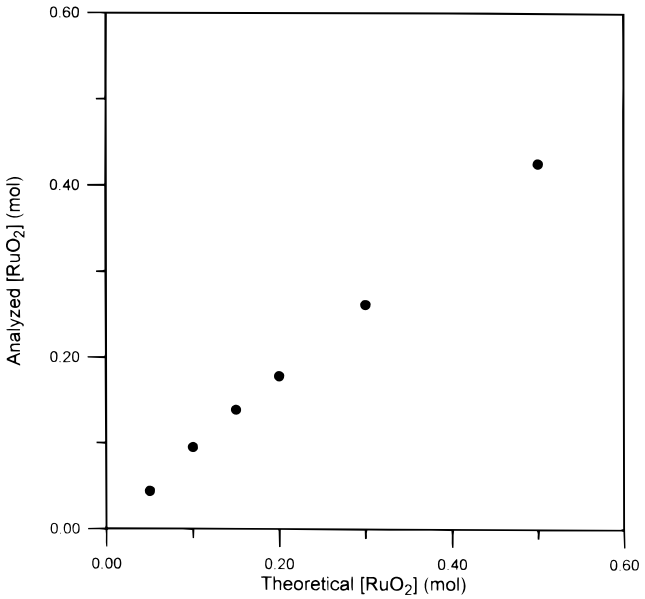

Figure 2. Analytical results by XRF of RuO_2 (mol) in previously milled pellets (fired at 1300 °C) versus theoretical content of RuO_2 (mol).

In this work, we demonstrate that the sol−gel process allows us to obtain more stable solid solutions in the TiO_2-RuO_2 system up to 600 °C. From 600 to 1300 °C, the extent of solid solubility is kept constant, although the RuO_2 that is not into the rutile lattice suffers a partial volatilization. It increases with a higher content of RuO_2.

C. Chemical Analysis. To minimize the RuO_2 volatilization, the samples were sintered by rapid firing. After sintering XRF chemical analysis was performed.

Before the chemical analysis was carried out, sintered samples were milled and homogenized. The resultant powders were pressed into pellets and were analyzed by XRF. Figure 2 shows the analyzed RuO_2 concentration versus theoretical RuO_2 content. These analyses indicated a partial volatilization of RuO_2 according to the DTA-TGA and XRD studies. That fact increases as RuO_2 concentration increases. A more detailed work on

(28) Ito, M.; Murakami, Y.; Kaji, H.; Ohkawauchi, H.; Yahikozawa, K.; Takasu, Y. *J. Electrochem. Soc.* **1994**, *141*, 1243.

(29) Bursill, L. A.; Hyde, B. G. *Progress in Solid State Chemistry*; Reiss, H., McCaldin, J. O., Eds.; Pergamon: Oxford 1972; Vol. 7, p 177.

(30) Veseloskaya, I. E.; Spasskaya, E. K.; Sololov, V. A.; Tkachenko, V. I.; Yakimenko, L. M. *Electrokhimiya* **1974**, *10*, 70.

(31) Hine, F.; Yasuda, M.; Yoshida, T. *J. Electrochem. Soc.* **1977**, *124*, 500.

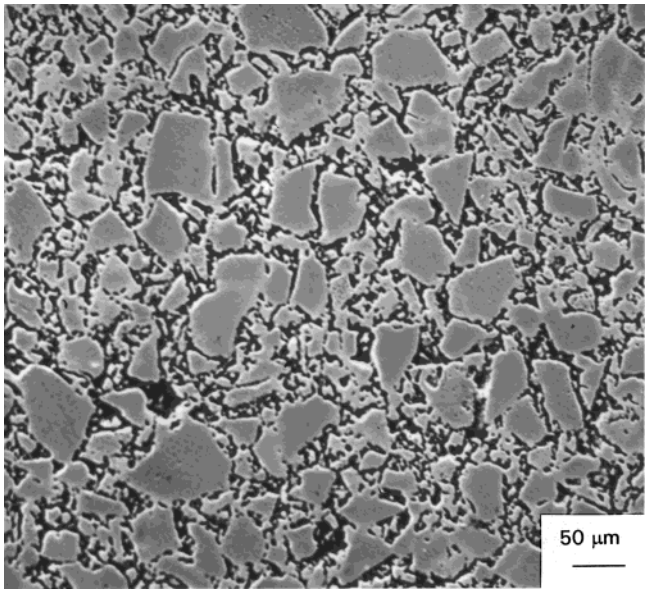

Figure 3. SEM micrograph of the polished surface of the sintered sample 90T10R.

this chemical analysis was reported elsewhere.[32]

Since the chemical analysis shows that a RuO_2 partial volatilization occurs, the solid solution limit at 1300 °C would occur in $0.045 \leq x < 0.095$ range.

D. SEM-EDX and TEM. By this route, nanometric, highly homogeneous and very reactive powders of rutile-type solid solutions can be obtained at low temperature. Agglomerates (50−80 nm) of very fine particles (~3 nm) are observed by TEM for the samples studied. A SEM micrograph of polished and chemically etched surface of the sintered 90T10R is shown in Figure 3. A monophasic morphology, constituted by big interconnected plates (30 μm), is noted. Inter- and intragranular porosity (black regions) is also noticed. The polished surface of 80T20R is shown in Figure 4. In this case, an interconnected net is perceived. In some regions free RuO_2 needles are also detected (Figure 5). Inter- and intragranular porosity is also noted. The big difference between both microstructures can be due to the RuO_2 to a typical mechanism of a second phase effect. When a second phase emerges, the grain growth of the main phase during the densification process is limited by the secondary phase. In our case, RuO_2 acts as a second phase which inhibits the growth of the TiO_2-RuO_2 solid solution (main phase). That fact can produce an interconnected net of irregular shape grains with intra- and intergranular porosity (see Figure 4). Relative densities of the studied materials are registered in Table 2. The chemical etching removes part of the material which result in an increase in the porosity of the samples compared to the ones measured in that table.

Similar microstructures to the 80T20R are observed for samples with higher RuO_2 contents, and then a higher number of RuO_2 regions are noted.

E. Electrical Transport Properties. *EIS (Semiconductor-Dielectric Regime, A).* In this section, the analytical values of RuO_2 content are considered. The nominal compositions are indicated in parentheses. Rutile-TiO_2 ($x = 0$) shows an impedance sole arc in the temperature range 250−1000 °C. TiO_2 is a typical insulator material with a very low conductivity at 50 °C (1.1×10^{-15} S cm^{-1}). Figure 6 shows the impedance spectra of the samples with $0.045\ (0.05) \leq x \leq 0.18\ (0.20)$ at 50 °C. A sole semicircle, which is associated with an equivalent circuit with resistance and capacitance in parallel, represents simultaneously both the bulk and the total conductivity contributions. In the studied

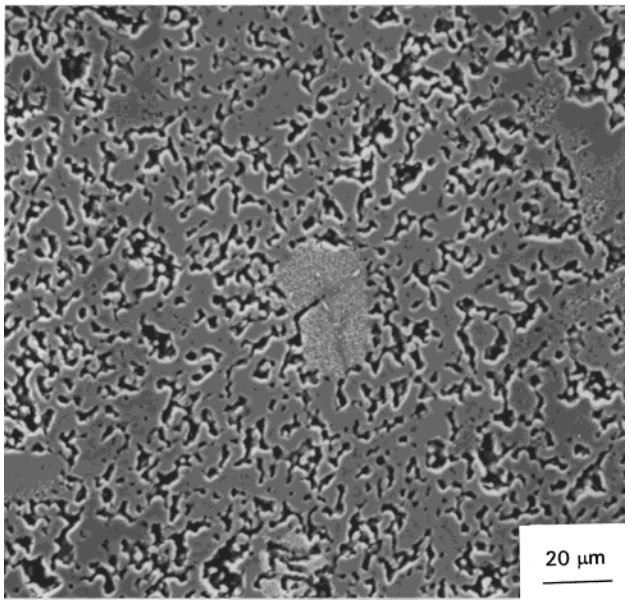

Figure 4. SEM micrograph of the polished surface of the sintered sample 80T20R.

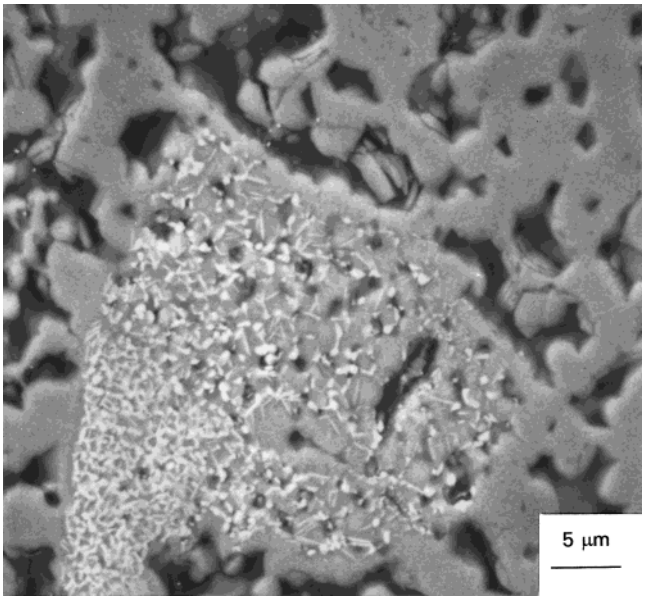

Figure 5. Detail of the micrograph of the sintered sample 80T20R.

Table 2. Relative Densities of the Sintered Bodies

nominal composition	relative density (%)
100T	99
95T5R	85
90T10R	81
85T15R	80
80T20R	78
50T50R	73
100R	61

(32) Colomer, M. T.; Valle, F. J.; Jurado, J. R. *Eur. J. Solid State Inorg. Chem.* **1997**, *34*, 85.

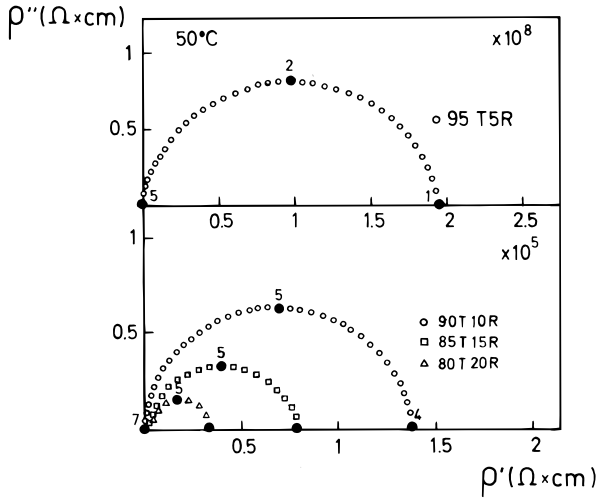

Figure 6. Impedance spectra of the samples with 0.045 (0.05) $\leq x \leq$ 0.18 (0.20) at 50 °C. Numbers above black spot are frequency logarithmic in hertz.

temperature range (room temperature to 500 °C), the observed sole arc vanishes and disappears when the temperature increases. The vanishing sole arc moves toward the right in the ρ' axis and finally disappears. The associated equivalent circuit changes as a function of temperature (see Figure 7). In both RuO_2 concentration and temperature dependence, when the sole arc disappears, an inductive loop simultaneously emerges. The associated equivalent circuit, in this case, is a resistance in series with a pseudoinductance that describes normally the behavior of metals, semimetals and also electrochemical interface effects, which take place, particularly, in corrosion processes.[33]

The temperature at which the equivalent circuit changes from an impedance arc to an inductive loop decreases as RuO_2 content increases. This critical temperature is labeled Tsp (semiconductor/pseudoinductance transition). The values of conductivity and its temperature trend (increasing conductivity as temperature is raised) correspond to a semiconductor regime. In Table 3, the conductivity at 50 °C, the Tsp and the energy gap values for these samples are registered.

The incorporation of RuO_2 in the lattice of rutile-TiO_2 shifts the Fermi level to the conduction band in TiO_2, as it is observed in Table 3. When TiO_2 is doped with 0.045 (0.05) mol of RuO_2, a sharp conductivity change of 7 orders of magnitude is noticed. Consequently, a donor level of 0.80 eV is created below the conduction band because a Rss is formed and the impurity band conduction (donor) can be the dominant mechanism. As RuO_2 content increases, RuO_2 phase is segregated. For instance, the 0.095 mol (90T10R) material conductivity increases 3 orders of magnitude (with respect to the 95T5R sample). The energy gap donor level is also reduced to 0.48 eV. Then, the conduction mechanism could be accounted for by two different associated transport processes: (i) due to the impurity band conduction mechanism and (ii) due to the fact that Rss grains and/or RuO_2 are very close each other. The electron hopping between equivalent Ru^{3+} and Ru^{4+} lattice sites could take place. The existence of Ru^{3+} was

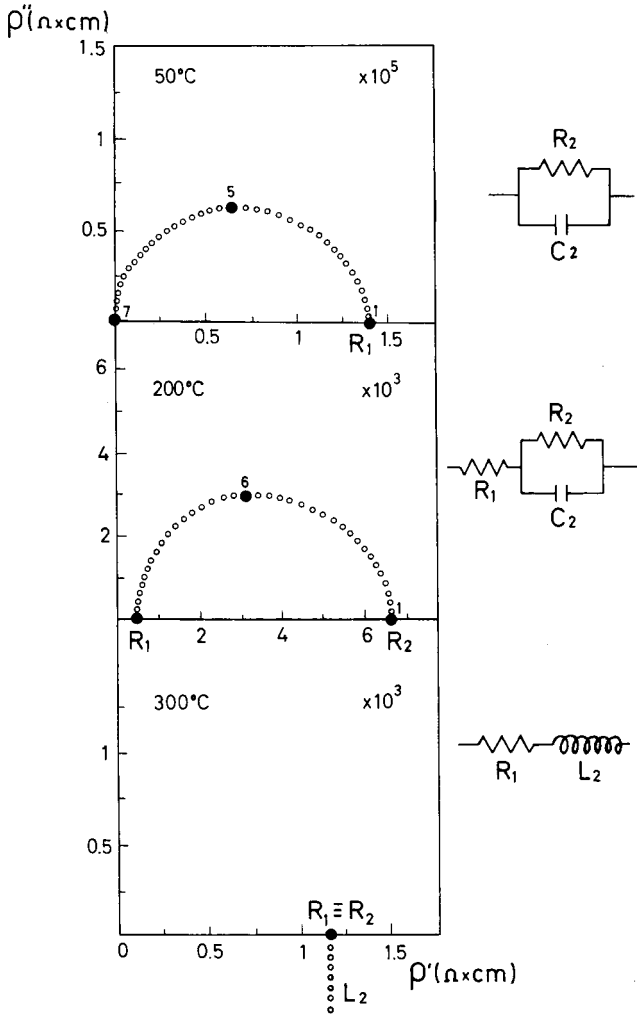

Figure 7. Impedance spectra and equivalent circuit at three different temperatures for the sintered sample 85T15R.

Table 3. Some Electrical Data of the Samples with 0 $\leq x \leq$ 0.18 (0.20) at 50 °C

nominal composition	$\sigma_{(50°C)}$ (S cm^{-1})	T_{sp} (°C)	energy gap (eV)
100T	1.1×10^{-15}[a]		3.20
95T5R	5.1×10^{-9}	500	0.80
90T10R	7.1×10^{-6}	300	0.48
85T15R	1.3×10^{-5}	285	0.44
80T20R	3.3×10^{-5}	250	0.38

[a] Extrapolated value.

detected elsewhere[27] by EPR in samples of the ZrO_2–Y_2O_3–RuO_2 system.

The decreasing of Tsp as RuO_2 concentration increases could indicate a sharp change of the electron mobility edge, and above Tsp, the increment of temperature can induce a band overlapping implying either metal/insulator Mott transition or narrow band transport behavior similar to that which takes place in some $LnCoO_3$ perovskites (Ln = La, Pr, Nd, Sm, Eu, and Gd).[34]

2. DC Four-Points Measurements. Electrical Conduction (Semiconductor/Metal Transition and Metallic Regimes (B and C, Respectively). When the RuO_2

(33) MacDonald, D. D. *J. Electrochem. Soc.* **1978**, *12*, 2062.

(34) Yamaguchi, S.; Okimoto, Y.; Tokura, Y. *Phys. Rev. B* **1996**, *54*, 54.

Table 4. Electrical Conductivity Values at 50 °C for Materials 0.26 (0.30) ≤ *x* ≤ 1

nominal composition	analyzed composition	$\sigma_{(50°C)}$ (S cm^{-1})
70T30R	74T26R	0.78
50T50R	57T43R	1.90
100R		1.12×10^3

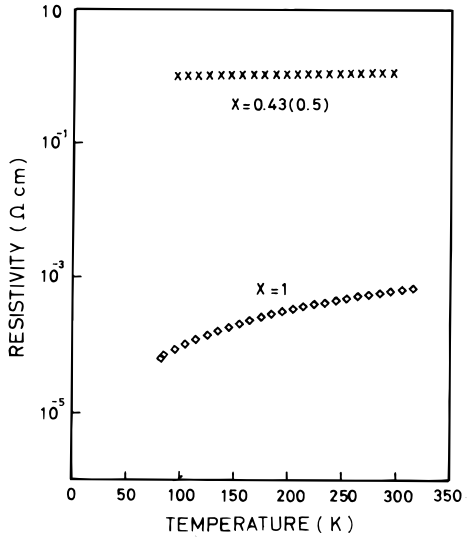

Figure 8. Resistivity versus temperature for $x = 0.43$ (0.50) and 1 mol.

concentration is higher than 0.18 (0.20) mol, the impedance spectroscopy measurements can be no longer used. The electrical conductivity was measured by the classical four-points method, since impedance spectroscopy analyses exhibit a pseudoinductance behavior in the whole studied temperature range. Table 4 shows the conductivity values, at 50 °C, of the materials with 0.26 (0.30) ≤ *x* ≤ 1.

The resistivity versus temperature plot, for $x = 0.43$ (0.50) and 1 mol, is shown in Figure 8. Both materials behave electrically as a metal. RuO_2 has a conductivity 4 orders of magnitude higher than that of $x = 0.43$ (0.50). It is due to the fact that the Rss acts as a blocking phase and it has a significant effect in the reduction of its metallic conductivity.

For 0.18 (0.20) < *x* < 0.26 (0.30), the semiconductor−metal transition could be established. The change of the conductivity values, in this concentration range, is wide and smooth (the conductivity values do not change significantly).

The obtained results in this work are discussed on the basis of the Percolation Theory.[35,36]

Figure 9 shows the variation of the conductivity, at 50 °C, as a function of the RuO_2 content. This curve agrees with the expected behavior for a mixture of semiconductor/conductor oxide phases.

Figure 10 plots the log σ versus $[RuO_2]^{-1}$. The experimental data fit two straight lines. Its intersection shows a critical value of 0.064 (mol %)$^{-1}$, which corresponds to a RuO_2 content of 0.16 mol. Above this value, the conductivity fits the percolation pattern well, and is deviated for lower amount of RuO_2. This critical value

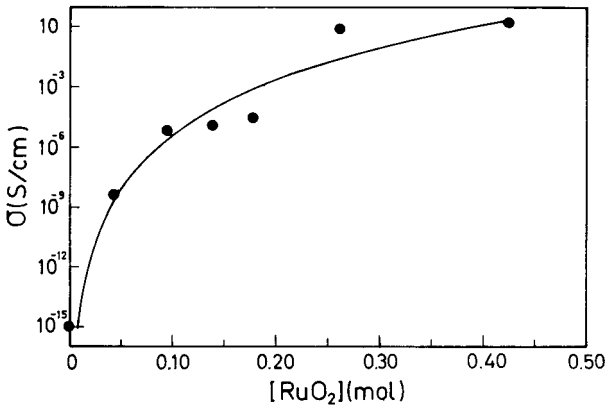

Figure 9. Conductivity at 50 °C as a function of the RuO_2 content ($0 \le x \le 1$).

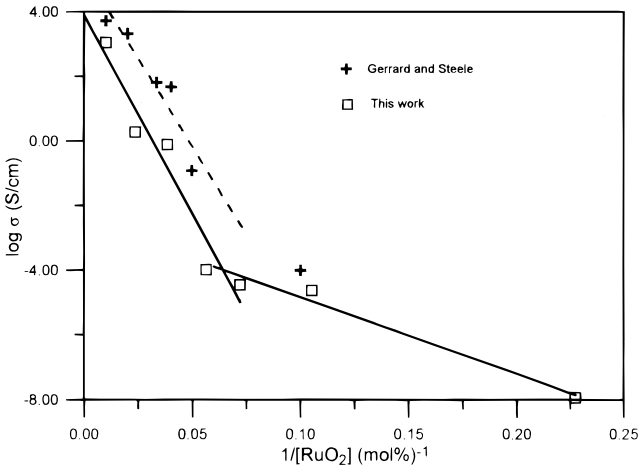

Figure 10. log conductivity of the sintered materials versus the reciprocal of RuO_2 content. Comparison between Gerrad and Steele's work (ref 10) and this study.

can indicate the initial step of ruthenium oxide metallic percolation. The semiconductor/metal transition is denoted from 0.16 to 0.26 mol. Above 0.26 mol, the materials are metallic in nature.

In films prepared at 400 °C, Gerrard and Steele[10] reported that the conductivity of the films fits the percolation pattern well, but they only prepared films from 10 mol % of RuO_2. They did not reported compositions with lower amount of RuO_2.

A more detailed view in Figure 10 of Gerrard and Steele's[10] work could indicate that they have similar results as this study. The percolation habit of both types of samples should be the same. Above the critical point of 0.16 mol RuO_2, the slopes of the straight lines are similar: −109.01 for Gerrard and Steele's work and −123.17 in this study. Probably, the slope is not equal, because these authors have not reported compositions lower than 10 mol % as it is mentioned above.

Conclusively, in this work, a wide transition ($0.16 \le x_c \le 0.26$) semiconductor/metal is established, which seems to indicate the presence of a prepercolation regime. This effect is not considered in the classical Percolation Theory.

3. Microstructural/Electrical Approach. By taking into account, the microstructural picture (Figure 11), and according to the obtained conductivity results, a microstructural/electrical approach is constructed. In

(35) Stinchombe, R. B. *J. Phys. Soc. C* **1974**, *7*, 179.
(36) Abeles, B.; Pinch, H. L.; Gittleman, J. L. *Phys. Rev. Lett.* **1975**, *35*, 247.

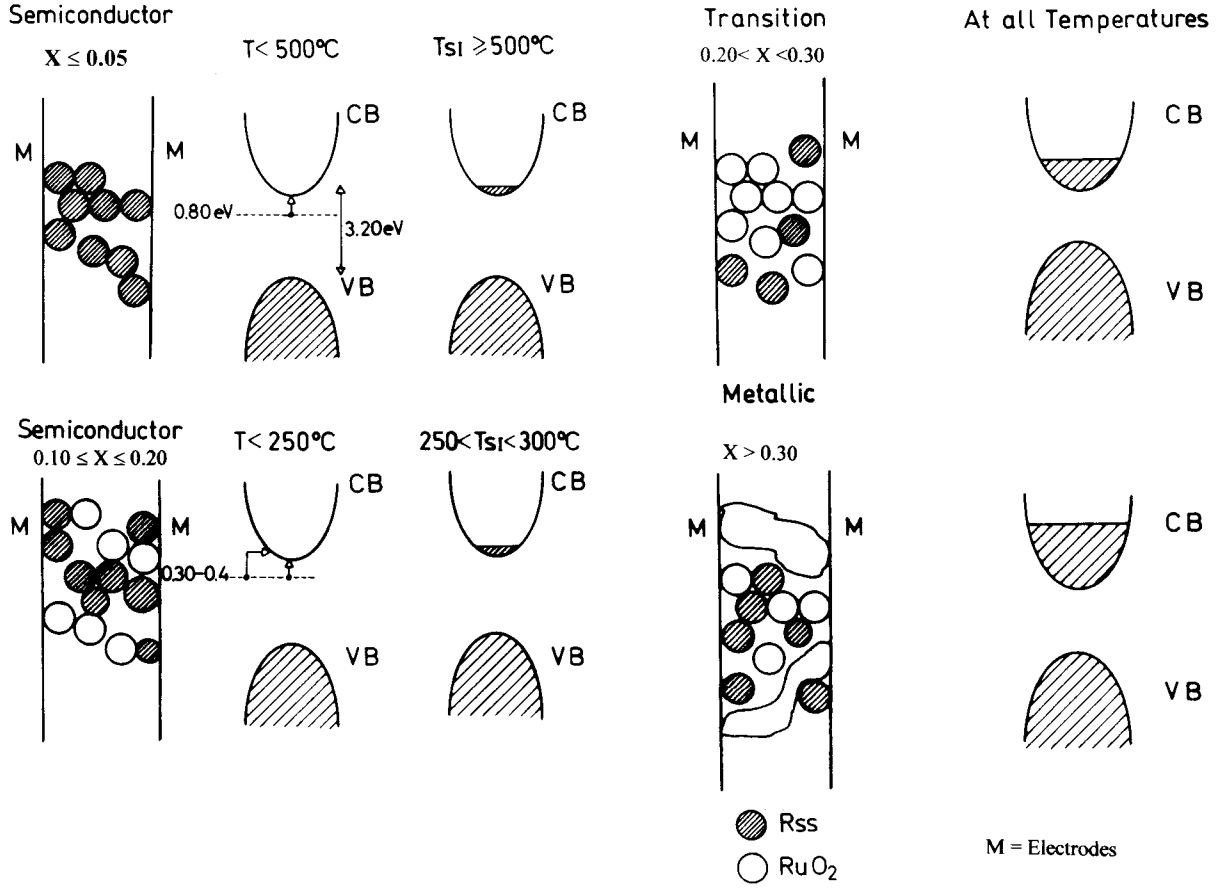

Figure 11. Microstructure/electrical picture in the TiO_2-RuO_2 system. Microstructure−electronic band approach. CB means conduction band and VB means valence band.

this approach, the percolation metal (RuO_2) behavior and its corresponding electronic band structure is considered.

(i) The microstructure of the sample with $x = 0.045$ (0.05) shows Rss grains where the electrons could jump from the valence to the conduction band with a donor level situated at 0.8 eV. TiO_2 (rutile) band feature indicates the presence of an empty conduction band. When RuO_2 is introduced (5 mol %), an impurity band conduction mechanism (IBC) could be noted, but from 500 °C the Rss behaves like a pseudoinductance and that could be indicating the presence of few electrons (temperature induced) in the conduction band. Simultaneously, a shifting of the band edges can also occur (Figure 11 does not consider this effect).

(ii) The presence of RuO_2 grains can also be taken into account in the electrical transport. Rss and RuO_2 can participate in the electron-hopping process $Ru^{4+} \rightarrow Ru^{3+} + 1e-$. So in that case, both IBC and electron hopping, yielded by Rss and/or RuO_2-separated grains, occur. At Tsp, the electron occupation density in the band conduction is increased as RuO_2 content increases.

(iii) The two phases, Rss and RuO_2, coexist and are clearly noted and both are participating in the electrical transport. The conduction band electron density is then much higher, the semiconductor behavior no longer takes place, and simultaneously the metallic regime starts.

(iv) The RuO_2 metallic phase is continuous and the Rss phase is now a blocking electron phase. This means that the material has a metallic behavior and now the conduction band electron density is high. The shifting of the band edges is also eliminated.

IV. Conclusions

1. Xerogels, nanoparticle powders, and ceramic bodies of all compositions studied in the TiO_2-RuO_2 system can be prepared by a polymeric sol−gel route.

2. At temperatures as low as 300 °C, $(Ti-Ru)O_2$ solid solutions with good crystallinity were attained. Although, from 300 to 500 °C, the solid solubility of RuO_2 in rutile-TiO_2 phase is located at $x \geq 0.50$, from 600 to 1300 °C, that value is located in the $0.05 \leq x < 0.10$ range. For higher contents of RuO_2, two phases are observed: ruthenium−titanium oxide rutile solid solution and RuO_2. The volatilization reaction in air could start at temperatures lower than 800 °C.

3. Two types of electrical behavior are observed in sintered materials of this system: semiconductor and metallic. RuO_2 is a metallic phase and $(Ti-Ru)O_2$ solid solution behaves as a semiconductor phase. A wide transition semiconductor/metal is noted ($0.16 \leq x_c \leq 0.26$), which indicates the existence of a prepercolation effect. The metal/electrical percolation could be located with a chemically analyzed composition of $x = 0.26$.

Acknowledgment. Authors are grateful for the financial support from EC Project (JOE3-CT97-0049) and CICYT-MAT Project 98-1467-CE and to Dr. F. J. Valle for the chemical analyses performed.

CM9903879